Anal Bioanal Chem (2015) 407:1567–1576
DOI 10.1007/s00216-014-8406-3

RESEARCH PAPER

Organically modified silica nanoparticles doped with new acridine-1,2-dioxetane analogues as thermochemiluminescence reagentless labels for ultrasensitive immunoassays

Massimo Di Fusco · Arianna Quintavalla · Marco Lombardo · Massimo Guardigli · Mara Mirasoli · Claudio Trombini · Aldo Roda

Received: 20 October 2014 / Revised: 4 December 2014 / Accepted: 10 December 2014 / Published online: 27 December 2014

Abstract Doped organically modified silica nanoparticles (ORMOSIL NPs) with luminescent molecules represent a potent approach to signal amplification in biomolecule labeling. Herein, we report the synthesis of new ORMOSIL NPs incorporating thermochemiluminescent (TCL) 1,2-dioxetane derivatives to prepare TCL labels for ultrasensitive immunoassay, displaying a detectability comparable to those offered by other conventional luminescence-based systems. Amino-functionalized ORMOSIL NPs were synthesized for inclusion of acridine-containing 1,2-dioxetane derivatives with a fluorescence energy acceptor. The doped ORMOSIL NPs were further functionalized with biotin for binding to streptavidin-labeled species to be used as universal detection reagents for immunoassays. A quantitative non-competitive immunoassay for streptavidin has been developed by immobilizing anti-streptavidin antibody to capture streptavidin, then the antibody-bound streptavidin was detected by the biotinylated TCL ORMOSIL NPs. The analytical performance was similar to that obtained by chemiluminescent (CL) detection using horseradish peroxidase (HRP) as label, being the limits of detection 2.5–3.8 and 0.8 ng mL^{-1} for TCL and CL detection, respectively. In addition, since the TCL emission is simply initiated by thermolysis of the label, chemical reagents were not required, thus allowing reagentless detection with a simplification of the analytical protocols. A compact mini dark box device based on the use of a cooled charge-coupled device (CCD) and a miniaturized heater has been developed and used to quantify the light emission after heat decomposition of the label at a temperature of 90–120 °C. These characteristics make TCL-doped ORMOSIL NPs ideal universal nanoprobes for ultrasensitive bioassays such as immuno- and DNA-based assay.

Keywords ORMOSIL nanoparticles · Thermochemiluminescence · 1,2-Dioxetanes · Biotin conjugation · Bioassays · Imaging

Introduction

The development of ultrasensitive and simple bioassays in miniaturized formats is one of the main trends in bioanalytical chemistry, owing to their great potential in clinical diagnostics, environmental monitoring, and food safety assessment. For these applications, highly sensitive detection principles are required, thus prompting the exploration of novel detection principles, molecules, materials, and analytical format. Among emission luminescence-based detection techniques, chemical luminescence such as chemiluminescence (CL), bioluminescence (BL), and electrogenerated chemiluminescence (ECL) has been shown to be particularly suited for these applications, offering high detectability even in low volumes, wide linear range of the response, and high signal/noise ratio [1, 2]. They have been employed in a variety of conventional and innovative analytical formats, such as microtiter plate, microfluidic devices, microarrays, lateral flow immunoassays, and paper-based devices [3]. Nevertheless, CL, BL, and ECL

Electronic supplementary material The online version of this article (doi:10.1007/s00216-014-8406-3) contains supplementary material, which is available to authorized users.

M. Di Fusco (✉) · M. Mirasoli
Advanced Applications in Mechanical Engineering and Materials Technology, Interdepartmental Center for Industrial Research, Alma Mater Studiorum, University of Bologna, Viale Risorgimento 2, 40136 Bologna, BO, Italy
e-mail: massimo.difusco@unibo.it

M. Di Fusco · A. Quintavalla (✉) · M. Lombardo · M. Guardigli · M. Mirasoli · C. Trombini · A. Roda
Department of Chemistry "G. Ciamician", Alma Mater Studiorum, University of Bologna, Via Francesco Selmi 2, 40126 Bologna, BO, Italy
e-mail: arianna.quintavalla@unibo.it

detection requires the addition of reagents (e.g., enzyme substrates and/or co-reactants) to elicit light emission, thus reducing assay rapidity and simplicity that are crucial for on-field applications. In addition, being such phenomena based on reactions occurring in solution, diffusion of reaction intermediates before light emission decreases signal spatial resolution with respect to fluorescence detection, which could be detrimental for microarray or microscope imaging applications.

Recently, thermochemiluminescence (TCL) detection, firstly described in 1963 [4] and proposed for analytical purposes in the late 1980s with little development and applications [4–6], was re-proposed by us as a promising detection technique, offering challenging and unexplored opportunities for ultrasensitive detection in bioanalysis [7, 8]. This detection principle, based on the use of molecules that undergo thermolysis upon heating with the formation of a product in a singlet excited state that decay with photon emission, shares the advantage of high signal-to-noise ratios with CL, BL, and ECL detection and presents additional appealing features for miniaturized analytical formats. In fact, being light emission simply triggered by heating, chemical reagents are not required to elicit photon emission, thus allowing reagentless detection. As in recent years a variety of miniaturized heating systems have been developed (e.g., for on-chip PCR) [9, 10], implementation of TCL-based detection in miniaturized bioanalytical devices appears to be technically feasible in short times.

We recently synthesized a series of acridine-containing 1,2-dioxetane derivatives (**1**–**7**, Fig. 1) [7, 8] that display significant advantages with respect to the TCL labels proposed in the past, such as relatively low trigger temperatures (below 100 °C) and improved detectability. We also provided preliminary evidence that signal amplification obtained by the use of 1,2-dioxetane-doped silica nanoparticles (NPs) provided a detectability still lower but comparable to horseradish peroxidase (HRP) detected by the luminol/H_2O_2/enhancer CL system [11]. Indeed, ultrasensitive chemical luminescence detection most often requires signal amplification, such as enzyme-based cyclic amplification for many CL systems, or the use of co-reactants, such as tripropylamine, for amplification of ECL emission from tris(2,2′-bipyridyl) ruthenium(II) used as a label.

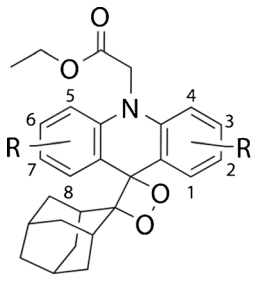

Fig. 1 Chemical structures of the TCL acridine-containing 1,2-dioxetane derivatives **1**–**7**

Indeed, doped silica NPs represent a convenient approach to signal amplification in biomolecule labeling [12–14], since silica NPs are easily synthesized, stable, optically transparent, water-compatible, heat-resistant, and can incorporate (depending on their size) up to tens of thousands of dyes or fluorophores, thus providing high signal amplification ensuring a large amount of label molecule/analyte molecule.

Herein, we report for the first time the synthesis of highly monodispersed and homogeneous organically modified silica (ORMOSIL) NPs incorporating the TCL molecules **1**–**7** with amino groups on the surface and demonstrate their suitability as highly detectable TCL nanoprobes for biospecific binding assays.

The doped ORMOSIL nanoparticle (ORMOSIL NP) synthetic procedure was optimized to obtain the highest TCL emission efficiency, then, after characterization, the NPs were functionalized with biotin to obtain a general purpose label able to bind any streptavidin-conjugated biospecific probe. Their analytical performance was evaluated in a non-competitive heterogeneous immunoassay for the detection of streptavidin as a model protein analyte, employing anti-streptavidin antibody immobilized on a glass solid support. To reach full assay portability, a compact battery-operated device, comprising an ultrasensitive thermoelectrically cooled CCD and a flat metal heater encased in Kapton for TCL emission trigger, was developed. The limit of detection obtained was similar to that achieved employing the CL system based on HRP label and luminol/hydrogen peroxide/enhancer cocktail, thus showing promising applications of TCL-doped NPs as universal labels in bioassays.

Materials and methods

Materials

The biotin-HRP conjugate, the CL substrate SuperSignal ELISA Femto, and the sulfosuccinimidyl-6-[biotin-amido]hexanoate (EZ-Link Sulfo-NHS-LC-Biotin) were purchased from Thermo Fisher Scientific (Waltham, MA, USA). All other reagents were purchased from Sigma-Aldrich Co. (St. Louis, MO) and used as received.

Synthesis of ORMOSIL NPs

Doped amino-containing ORMOSIL NPs were prepared by adapting a previously reported procedure [12, 15] via the hydrolysis of triethoxyvinylsilane (TEOVS) and (3-aminopropyl)triethoxysilane (APTES), [3-(2-aminoethylamino)propyl]trimethoxysilane (AEAPS), or 3-[2-(2-aminoethylamino)ethylamino]propyltrimethoxysilane (AEEAPS) in the non-polar core of dioctyl sodium sulfosuccinate (Aerosol-OT)/1-butanol/water micelles. The

micelles were obtained by dissolving the surfactant Aerosol-OT (0.22 g) and the co-surfactant 1-butanol (400 μL, 0.28 g) in deionized water (10 mL) by vigorous magnetic stirring. Then, a dichloromethane solution (50 μL) containing the 1,2-dioxetane derivative (1 mg) and 9,10-bis(phenylethynyl)anthracene (BPEA, 0.25 mg) or dipyridamole (DP, 1 mg) was added to the micellar solution, followed by neat TEOVS (100 μL). Void NPs were obtained using the same procedure except that neat dichloromethane (50 μL) was added to the micellar solution. The resulting solution was stirred for about 30 min, then neat (trialkoxy)alkylaminosilane (50 μL) was added and the solution was again stirred for about 20 h. The entire reaction was carried out at room temperature. The NPs were purified by dialysis against deionized water for 2 days at 4 °C using 12–14 kDa molecular weight cutoff (MWCO) dialysis tubing cellulose membranes (Spectra/Por® Dialysis Tubing) with a width of 25 mm. The dialyzed suspension was finally filtered through a 0.2-μm cutoff membrane filter (Phenex™-RC). The obtained NPs had a final concentration of 3 mg mL^{-1} and were stored at −18 °C upon addition of 1 % (*v*/*v*) PEG300.

Conjugation of ORMOSIL NPs with biotin

In a typical procedure [16], purified amino-containing ORMOSIL NPs suspension (1 mL) was mixed with PBS (10 μL, 1.0 mol L^{-1}, pH 7.4) to obtain a final suspension of NPs in 0.01 mol L^{-1} PBS, pH 7.4. A solution of sulfosuccinimidyl-6-[biotin-amido]hexanoate (EZ-Link Sulfo-NHS-LC-Biotin) (1 mg) in water (50 μL) was added to the NPs suspension and the mixture was stirred for 1 h. The entire reaction was carried out at room temperature. The NPs were then purified by dialysis against deionized water for 3 days at 4 °C using 12–14 kDa MWCO dialysis tubing cellulose membranes (Sigma-Aldrich Co.) with a width of 10 mm. The biotinylated ORMOSIL NPs were used immediately after dialysis or stored at −18 °C upon addition of 1 % (*v*/*v*) PEG300.

ORMOSIL NPs characterization

Transmission electron microscopy (TEM)

Bright-field TEM images were acquired using a Philips CM100 transmission electron microscope (Philips/FEI Corp., Eindhoven, Holland). A drop of the NPs suspension was transferred onto porous carbon foils supported on conventional copper microgrids without any additional treatment. The ORMOSIL NPs size distribution was obtained by measuring the size of about 100 NPs for each sample using MetaMorph image analysis software (Molecular Devices, LLC, Sunnyvale, CA).

Determination of entrapment efficiency of compounds **1–4** *in ORMOSIL NPs*

In a typical experiment, an aliquot (500 μL) of a suspension of ORMOSIL NPs containing the 1,2-dioxetane derivatives **1**–**4** and BPEA (ORMOSIL/**1**–**4**/BPEA NPs) was filtered by centrifugation filter membranes (100-kDa cutoff, Merck Millipore) before dialysis to separate the NPs. The amounts of compounds **1**–**4** and BPEA in the filtrate were determined by comparing the absorption spectrum of the filtrate with those of standard solutions of the compounds.

Spectrophotometric assay for the determination of surface-available biotin

A biotin calibration curve was prepared by adding known amounts of biotin to a test solution containing 10 nmol mL^{-1} streptavidin and 50 nmol mL^{-1} 2-(4-hydroxyphenylazo)benzoic acid (HABA) in PBS (0.1 mmol L^{-1}, pH 7.4) and measuring the changes in the absorbance due to the displacement of the dye from streptavidin [17]. A Varian Cary 50 Scan UV-Visible spectrophotometer (Varian Inc., Palo Alto, CA) was used for spectrophotometric measurements. Then, different aliquots of biotin-conjugated void ORMOSIL NPs were mixed with the HABA-streptavidin test solution (1 mL). The experiments were carried out using biotinylated void ORMOSIL NPs to avoid interference from BPEA, which absorbs at the same wavelength (500 nm) of the dye-streptavidin complex. Surface-available biotin (μg biotin per mg NPs) was calculated based on the decrease in absorbance at 500 nm using the equations reported in ref. [17].

TCL device

A compact imaging system, controlled by a laptop computer, was built by employing a portable battery-operated CCD camera (model MZ-2PRO, MagZero, Pordenone, Italy) equipped with a thermoelectrically cooled monochrome CCD image sensor [18–20]. The camera was coupled with an objective (low distortion wide angle lenses 1/3 in. 1.28 mm, f1.8) obtained from Edmund Optics (Barrington, NJ) and connected to a light-tight dark box. The inner surface of the dark box top cover was equipped with a flat heating element (20×20 mm^2), comprising a serpentine nickel/chrome thin-film resistance (79.5Ω) encased in kapton, and clamps to hold 20×20-mm^2 glass slides in contact with the heater (Fig. 2). The heater was powered by the CCD battery and, with the use of a manually regulated resistor, the appropriate voltage was applied to reach the required temperature (e.g., 4.5 V for a 120–140 °C temperature). Thanks to its light reflecting properties, the metal heater also increased the fraction of emitted photons that could reach the CCD sensor. Images, acquired employing 1-min integration

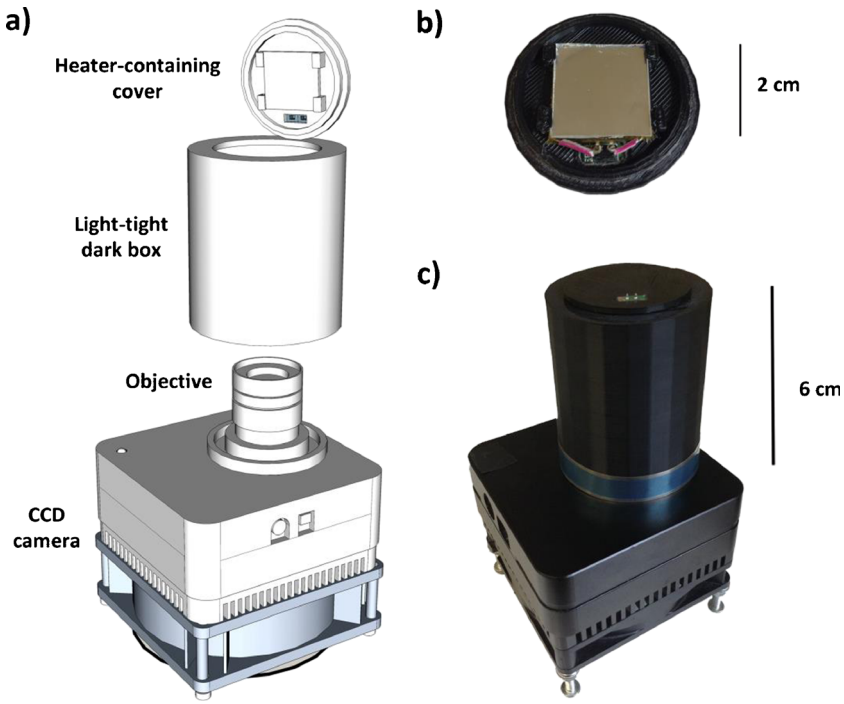

Fig. 2 **A** Scheme of the portable imaging device. **B** Heater-containing cover. **C** The CCD camera/dark box/heater-containing cover assembly

time, were recorded in the Flexible Image Transport System (FITS) format and analyzed with the WinLight 32 software version 2.91 (Berthold Technologies GmbH & Co. KG, Bad Wildbad, Germany).

For reference, a research-grade luminograph (NightOWL LB 981, Berthold Technologies GmbH & Co. KG) equipped with a back-illuminated, thermoelectrically cooled CCD camera was also employed. In this case, microscope glass slides glued to a 50×70-mm^2 flat heating element were employed as a solid support. The temperature of the support was varied by applying a suitable current and monitored by a copper/constantan thermocouple. Image integration times varied from 5 to 30 s (for evaluation of TCL decay kinetics) to 5 min (for stability measurements).

TCL light emission measurements

TCL decomposition kinetic measurements

The TCL emission decay kinetics were measured by spotting small amounts of compounds **1**–**7** (1 μL of 1 mg mL^{-1} acetonitrile solution) or doped ORMOSIL NPs (1 μL of 3 mg mL^{-1} water suspension) onto a microscope glass slide. The spots were allowed to dry, then the slide was heated to the desired temperature (in the range between 70 and 140 °C), and a sequence of images of the TCL emission was acquired with the NightOWL LB 981 luminograph. For each temperature, the kinetic constant k of the TCL process was calculated by fitting the decay profile of the TCL emission with the first-order decay equation shown in Eq. 1

$$I_{TCL} = (I_{TCL})_0 e^{-kt} \quad (1)$$

in which I_{TCL} is the TCL signal at time t and $(I_{TCL})_0$ is the TCL signal at time zero. Then, the activation energy E_a and the pre-exponential factor A of the TCL process were calculated from the kinetic constants k measured at different temperatures using the logarithmic form of the Arrhenius equation (Eq. 2)

$$lnk = lnA - \left(\frac{E_a}{RT}\right) \quad (2)$$

in which R is the universal gas constant and T is the temperature. Kinetic measurements at room temperature were performed in black 96-well microtiter plates covered with an adhesive transparent plastic foil to avoid solvent evaporation. Measurements were performed in acetonitrile (20 μL of a 0.1 mg mL^{-1} solution of 1,2-dioxetane) and water (20 μL of a solution prepared by adding 50 μL of a 2-mg mL^{-1} solution of 1,2-dioxetane in acetonitrile to 950 μL of water).

Thermal stability measurements

The stability of the ORMOSIL/**1**–**4**/BPEA NPs stored in different conditions (at +4 °C in water and at −18 °C in water containing 1 % (*v*/*v*) PEG300), and TCL measurements were performed at 1-week intervals during 30 days. In details, aliquots of NP suspensions (1 μL) were deposited onto glass supports with a micropipette, and the TCL signal was acquired with the NightOWL LB 981

luminograph while heating the support to 120 °C using an integration time of 5 min.

TCL immunoassay for the detection of streptavidin

Glass supports (20×20 mm^2) were cut from amino-functionalized glass slides (Sigma-Aldrich Co.), then treated with glutaraldehyde (5 % (*v*/*v*)) in carbonate buffer (0.1 mol L^{-1}, pH 9.0) for 4 h, washed with absolute ethanol (three times) and deionized water (three times), and air-dried at room temperature. Anti-streptavidin antibody was immobilized onto the slides by depositing an array of 1-μL spots of the antibody solution in carbonate buffer (0.1 mol L^{-1}, pH 9.0). The slides were incubated at 4 °C overnight in a humid chamber, then washed three times with PBS (0.1 mol L^{-1}, pH 7.4) containing Tween-20 (0.1 % (*v*/*v*)) and rinsed with abundant deionized water. Afterwards, streptavidin solutions (2 μL) in PBS (0.1 mol L^{-1}, pH 7.4) at different concentrations (ranging from 1 to 500 ng mL^{-1}) were deposited onto the slides in correspondence of the spots of anti-streptavidin antibody and incubated 2 h at room temperature in a humid chamber. The slides were washed three times with PBS (0.1 mol L^{-1}, pH 7.4) containing Tween-20 (0.1 % (*v*/*v*)) and rinsed with abundant deionized water.

For TCL detection, a suspension of Biot-ORMOSIL/**1**–**4**/BPEA NPs (10 μL) in PBS (0.005 mol L^{-1}, pH 7.4) was deposited onto the slides in correspondence of the spots containing the antibody–antigen complexes with the help of a homemade PDMS mold and incubated overnight at 4 °C in a humid chamber. The slides were washed three times with PBS (0.1 mol L^{-1}, pH 7.4) containing Tween-20 (0.1 % (*v*/*v*)), rinsed with abundant deionized water to eliminate the excess of Biot-ORMOSIL NPs, and almost dried at the air before the measurements. Then, the TCL signals were measured upon heating the glass slide to 120 °C by acquiring a TCL image of the array of spots with the portable CCD-based device using an acquisition time of 1 min.

For CL detection, a solution of biotin-conjugated HRP (10 μL) was deposited onto the slides instead of Biot-ORMOSIL/**1**–**4**/BPEA NPs and incubated 2 h at room temperature in a humid chamber. The slides were washed three times with PBS (0.1 mol L^{-1}, pH 7.4) containing Tween-20 (0.1 % (*v*/*v*)) and rinsed with abundant deionized water. Then, the HRP CL substrate SuperSignal ELISA Femto (70 μL) was dispensed onto the glass slide and distributed with the help of a coverslip glass slide. The resulting CL signal was imaged with the portable CCD-based device using an acquisition time of 1 min.

To estimate the assay accuracy, a series of independently prepared streptavidin solutions in the range 10–400 ng mL^{-1} has been prepared in PBS (0.1 mol L^{-1}, pH 7.4) and analyzed both by TCL and CL detection.

Results and discussion

ORMOSIL NPs preparation

The synthetic procedure for the production of doped ORMOSIL NPs has been optimized using the 1,2-dioxetane derivative **1** as a model compound. As it has been reported that amines promote decomposition of the 1,2-dioxetane ring by both electron transfer [21] and nucleophilic attack [22], the main challenge was to avoid decomposition of the 1,2-dioxetane derivatives during the NPs preparation. We therefore investigated the use in the synthesis of ORMOSIL NPs of different (trialkoxy)alkylaminosilanes, namely APTES, AEAPS, and AEEAPS (Fig. 3A), and evaluated their effect on the TCL emission. As shown in Fig. 3B, the TCL signal intensity varied with the nature of the (trialkoxy)alkylaminosilane in the order AEEAPS > AEAPS > APTES. Assuming that the NPs obtained with the three aminosilanes have similar dimensions, such behavior can be reasonably ascribed to the different hydrophilicity of alkylamino side chains, which follow the trend *N*-*n*-propyldiethylenetriamine > *N*-*n*-propylethylenediamine > *n*-propylamine [23]. Indeed, a less hydrophilic side chain can easily penetrate into the hydrophobic core of the micelles [24] and promote the decomposition of the 1,2-dioxetane derivatives by electron transfer or nucleophilic attack, thus explaining the trend of TCL signal intensities.

An increase in the TCL emission can be obtained by entrapping in the doped ORMOSIL NPs, together with the 1,2-dioxetane derivatives, a fluorescence energy acceptor that could intercept those electronically excited states that undergo non-radiative decay processes, such as the triplet excited state. Two different energy acceptors were evaluated, namely BPEA and DP, which display very high fluorescence quantum yields (1.0 in cyclohexane [25] and 0.95 in a water solution at pH 7.0 [26], respectively) and absorption spectra that fairly well overlap with the TCL emission spectra of compounds **1**–**7** [8]. As shown in Fig. 3C, the addition of BPEA and DP significantly increased (up to five times) the TCL signal intensity with respect to the NPs without fluorescence energy acceptor. BPEA was slightly more effective, and it was therefore selected for further experiments. In addition, BPEA is highly hydrophobic, which should prevent its possible release from ORMOSIL NPs into the water medium.

The TCL emission of doped NPs was evaluated by acquiring a spectrum between 400 and 700 nm (see Electronic Supplementary Material (ESM) Fig. S23) upon heating at 90 °C an aliquot of ORMOSIL/**1**/BPEA NPs. As it can be seen, the TCL spectrum presents both the fluorescence

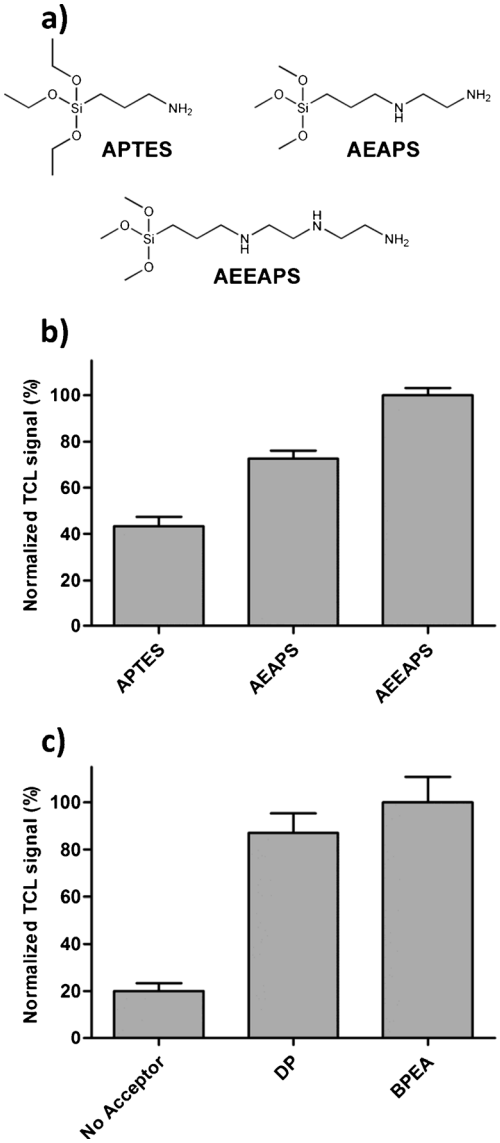

Fig. 3 **A** Chemical structures of the (trialkoxy)alkylaminosilanes used in the synthesis of ORMOSIL NPs. **B** Normalized TCL signals obtained for ORMOSIL/**1** NPs synthesized using APTES, AEAPS, or AEEAPS. **C** Normalized TCL signals obtained using ORMOSIL/**1**, ORMOSIL/**1**/DP, and ORMOSIL/**1**/BPEA NPs

emission of BPEA and the TCL emission of **1** with a maximum centered at 477 nm.

In addition, TCL compound **1** in ORMOSIL NPs doped with BPEA acceptor displayed TCL quantum yield in the same order of magnitude as compared with the conventional reference CL luminol/HRP/enhancer system.

ORMOSIL NPs doped with compounds **1–7** and BPEA (ORMOSIL/**1–7**/BPEA NPs)

TCL measurements showed that ORMOSIL/**1–4**/BPEA NPs were strongly luminescent, while only weak signals were observed for ORMOSIL/**5–7**/BPEA NPs. This outcome can be ascribed to the almost complete decomposition of the 1,2-dioxetanes by water [27] in the first stage of the NPs' growth, when it can diffuse towards the micelle cores [28–30], thus resulting in the failure of entrapping compounds **5–7** in the ORMOSIL NPs. To prove this assessment, we studied the TCL decay kinetics at 25 °C of compounds **1–7** both in water and acetonitrile (as a non-protic medium). The measurements in acetonitrile revealed very weak signals from compounds **5–7** (compounds **1–4** did not emit at room temperature), whereas in water, all the 1,2-dioxetane derivatives showed light emissions with half-lives ($t_{1/2}$) ranging from minutes for compounds **5–7** to hours for compounds **1–4** (ESM Table S1).

Entrapment efficiencies of 50–75 and 90 % were calculated for compounds **1–4** and BPEA, respectively (the lower entrapment efficiency of 1,2-dioxetane derivatives was probably still due to a partial water-promoted decomposition). We also calculated the loadings of 1,2-dioxetane derivatives and BPEA in NPs (the concentration of NPs was estimated from their weight and size assuming a density similar to that of silica, i.e., 2.2 g cm^{-3}). As a result, each NP roughly contained 850–1,300 molecules of 1,2-dioxetane derivatives **1–4** and 450 molecules of BPEA.

The morphological characterization of ORMOSIL/**1**/BPEA NPs was carried out by TEM imaging. The NPs appeared spherical and well dispersed in solution (Fig. 4A) and showed a nearly Gaussian particle size distribution with an average diameter of 32±6 nm (Fig. 4B).

Thermal decomposition activation parameters and stability of ORMOSIL/**1–4**/BPEA NPs

Upon heating at temperatures above 60 °C, TCL emissions with first-order decay kinetics were observed for compounds **1–4** both in the solid state and in ORMOSIL NPs. Table 1 shows the activation energies (E_a) and pre-exponential coefficients (A) of the TCL reactions. The activation energies of compounds **1–3** measured into ORMOSIL NPs were lower than in the solid state. This behavior has already been reported for compound **1** in a previous work [7], and it is in line with literature data suggesting that silica may catalyze the decomposition of 1,2-dioxetanes containing aromatic moieties [31]. Surprisingly, for compound **4**, i.e., the 1,2-dioxetane derivative having a methyl group onto position 4 of the acridine moiety, the activation energy of the TCL reaction was much higher in ORMOSIL NPs than in the solid state. This aspect needs further investigations that are underway in our laboratories.

We measured the stability of ORMOSIL/**1–4**/BPEA NPs over a period of 30 days of storage at +4 °C in water

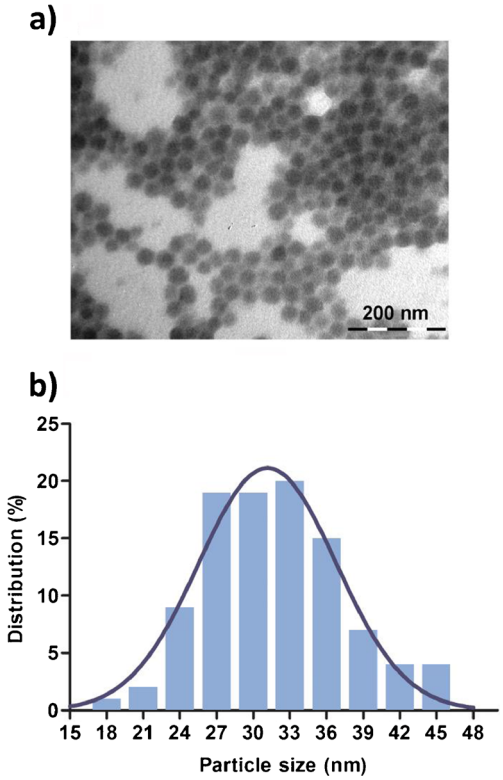

Fig. 4 **A** Representative TEM image of ORMOSIL/**1**/BPEA NPs and **B** particle size distribution obtained from the analysis of TEM images. The *line* represents the fitting of the particle size distribution with a Gaussian equation

and at −18 °C in water (added of 1 % (*v*/*v*) PEG300 to avoid freezing of the suspension and NPs coagulation). As expected from the activation energies of the TCL reactions, the ORMOSIL/**4**/BPEA NPs showed the highest stability, and their TCL signals decreased by 40 and 27 % after a 30-day storage at +4 and −18 °C, respectively. The decreases of TCL signal observed for ORMOSIL/**1**–**3**/BPEA NPs were much higher, ranging from 60 to 90 % and from 35 to 50 % at +4 and −18 °C, respectively (see ESM).

Table 1 Activation parameters for the TCL reactions of compounds **1**–**4** in the solid state and in ORMOSIL/**1**–**4**/BPEA NPs

Compound	Solid state		ORMOSIL NPs	
	E_a (kcal mol^{-1})	ln$A$	E_a (kcal mol^{-1})[a]	ln$A$[a]
1	29.7±1.2[b]	38.5±1.7[b]	26.9±1.7	30.1±4.4
2	25.7±1.6[c]	30.9±1.9[c]	22.0±0.2	24.6±0.3
3	24.5±0.3[c]	28.1±0.1[c]	23.7±1.5	26.2±3.8
4	23.0±0.4[c]	26.2±0.6[c]	28.0±1.5	31.7±1.7

[a] Mean±SD of four independent measurements

[b] Reference [7]

[c] Reference [8]

Biotin-modified ORMOSIL/**1**–**4**/BPEA NPs (Biot-ORMOSIL/**1**–**4**/BPEA NPs)

To obtain versatile detection reagents of general use for TCL-based bioassays, amino-modified ORMOSIL/**1**–**4**/BPEA NPs were further functionalized with biotin to develop a reagent that allows detection of both streptavidin- and biotin-labeled biospecific probes (the latter through formation of an intermediate streptavidin bridge).

Biotinylation of ORMOSIL NPs was performed using sulfosuccinimidyl-6-[biotin-amido]hexanoate, which provided a long spacer arm (22.4 Å) to reduce steric hindrance for biotin binding to streptavidin. The degree of biotinylation of ORMOSIL NPs, assessed by a spectrophotometric biotin assay [17], showed an amount of surface-available biotin equal to 6±1 μg mg^{-1} of NPs, corresponding to 545±90 biotin molecules per NP.

Portable device for TCL measurements

The developed compact and portable device is based on a monochrome back-illuminated thermoelectrically cooled CCD camera, displaying high quantum efficiency in the visible light range. We previously demonstrated its adequate analytical performance in terms of signal detectability and linear range, as well as spatial resolution, when used for BL/CL-based bioassays, either in conventional optics-based [19] or lensless contact imaging configurations [20, 32]. In the present configuration, the CCD was shown to be able to image a 20×20-mm^2 field at a 20-mm working distance, with sufficient spatial resolution and low cross-talk for accurate TCL measurements from 1-mm-diameter spots arrayed at a 2-mm spot-to-spot distance.

Calibration curves produced with compound **1** showed excellent light detectability, at the same level of that obtained with reference NightOWL LB 981 luminograph.

The optimal measurement conditions, providing the highest acquired signal with reasonable acquisition time, were assessed. As shown in Fig. 5, we observed, as expected, that the rate of decomposition increased with increasing the trigger temperature, although total TCL signal was not affected. Therefore, TCL measurements were performed at 120 °C to achieve the complete decomposition of the 1,2-dioxetane derivative within a 1-min integration time.

The signal-to-noise ratio of the CCD camera is independent from the working temperature of the TCL measurements due to an optimized distance of the CCD sensor (6 cm) from the heating element (Fig 2). However, the signal-to-noise ratio of the CCD camera is related to the working temperature of the sensor (cooled at −10 °C) [18] that remained constant during the measurements.

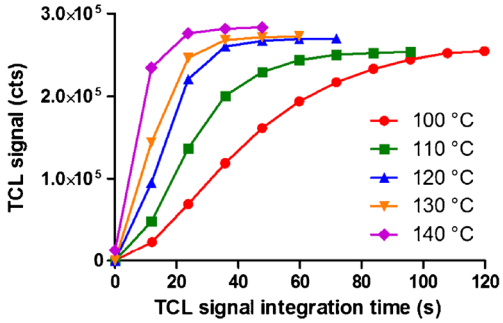

Fig. 5 TCL signals obtained for ORMOSIL/**1**/BPEA NPs by heating at different temperatures and employing different signal integration times

TCL immunoassay for the detection of streptavidin

The suitability of doped ORMOSIL NPs as labels for TCL-based ultrasensitive bioassays was evaluated in a model heterogeneous non-competitive immunoassay, in which streptavidin (used as analyte) was captured by anti-streptavidin antibodies immobilized onto the surface of glass slides and revealed by TCL imaging upon binding to Biot-ORMOSIL/**1**–**4**/BPEA NPs as TCL detection reagents.

A typical immunoassay calibration curve is reported in Fig. 6A. The calibration curve showed a good correlation between the TCL signal and the concentration of streptavidin in the range 4.0–500 ng mL^{-1} as shown in Eq. 3 where Y is the mean TCL signal of the spots and X is the concentration of streptavidin.

$$Y = (2,004 \pm 92)\log X - (124 \pm 159)\left(n = 7, R^2 = 0.990\right) \quad (3)$$

The assay showed a satisfactory reproducibility, displaying a CV lower than 15 % (evaluated on six replicates for each point). The limits of detection (LOD) of the immunoassay, defined as the amount of analyte giving a TCL signal higher than the blank signal plus three times its standard deviation, were in the nanogram per milliliter range (corresponding to approximately 10 amol of protein) for all the Biot-ORMOSIL/**1**–**4**/BPEA NPs (Table 2). Under these conditions, we can potentially detect a similar amount of any target analyte by an immunoassay exploiting the biotin-streptavidin system in a sandwich-type format.

For comparison, a calibration curve was also obtained by detecting the captured streptavidin by CL imaging upon addition of a biotin-HRP conjugate followed by a luminol-based CL substrate (Fig. 6A). Even in this case, a good correlation was observed between the mean CL signal of the spots (three replicates, CV lower than 12 %) and the concentration of streptavidin (Eq. 4).

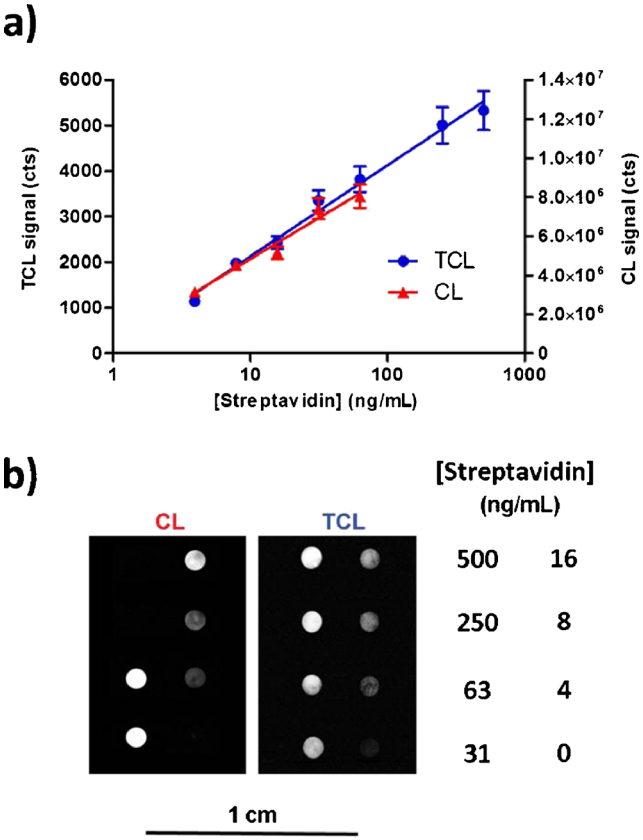

Fig. 6 **A** Comparison of the calibration curves obtained for the model immunoassay using TCL (Biot-ORMOSIL/**3**/BPEA NPs used as detection reagent) and CL imaging detection. **B** Images of CL and TCL emissions from an array of spots incubated with different concentrations of streptavidin. CL signals for 500 and 250 ng/mL of streptavidin were not shown due to the saturation of the CCD detector

$$Y = \left(4.21 \times 10^6 \pm 4.4 \times 10^5\right)\log X - \left(6.3 \times 10^5 \pm 5.6 \times 10^5\right) \quad (4)$$
$$\left(n = 5, R^2 = 0.968\right)$$

The LOD of the model immunoassay obtained with CL imaging detection (defined as reported above) was 0.8± 0.1 ng mL^{-1}, thus demonstrating that the detectability of the TCL imaging immunoassay based on Biot-ORMOSIL/**1**–**4**/BPEA NPs was comparable to that achievable with conventional enzyme-catalyzed CL imaging detection.

Table 2 Limits of detection for the immunoassay obtained using Biot-ORMOSIL/**1**–**4**/BPEA NPs as TCL detection reagents

TCL detection reagent	LOD (ng mL^{-1})[a]
Biot-ORMOSIL/**1**/BPEA NPs	2.9±0.5
Biot-ORMOSIL/**2**/BPEA NPs	2.6±0.3
Biot-ORMOSIL/**3**/BPEA NPs	2.5±0.3
Biot-ORMOSIL/**4**/BPEA NPs	3.8±0.4

[a] Mean±SD of six independent measurements

A series of independently prepared streptavidin solutions in the range 10–400 ng mL^{-1} have been also analyzed in order to estimate assay accuracy. The comparison of the results obtained either by TCL or CL detection with the expected values showed that the two assays displayed similar recovery, namely 90±5 and 93±6 %, respectively.

Conclusions

A simple and reproducible synthesis of novel biotin-functionalized ORMOSIL NPs doped with compounds **1**–**4** and the fluorescence energy acceptor BPEA (ORMOSIL/**1**–**4**/BPEA NPs) was reported, with the aim to obtain highly detectable amplified TCL labels for bioassays.

The nature and amount of (trialkoxy)alkylaminosilanes were optimized to obtain ORMOSIL NPs characterized by the highest loading of the 1,2-dioxetane derivatives and a relatively high surface density of amino groups. Inclusion of the fluorescence energy acceptor BPEA further increased TCL emission efficiency and intensity. Spherical NPs with a mean diameter of 32±6 nm were obtained, showing a narrow distribution in size and high stability when stored at −18 °C.

The possibility to label each biospecific probe (e.g., antibody) with a NP containing up to 1,000 TCL molecules provides signal amplification, similarly to what happens with enzyme-catalyzed reactions, in which excess of substrate ensures the reaction product accumulation. In future works, new NPs synthetic strategies will be pursued, e.g., employing different materials, in order to further increase the loading capacity.

The relatively low trigger temperature represents an enormous advantage over previously described TCL molecules, since it opens a wide variety of applications employing materials and supports commonly employed in bioanalysis. Indeed, in this work, a portable cooled CCD-based device for TCL imaging measurements was developed, which includes a thin film resistance for controlled heating of the analytical solid support (glass slide in this work) and an ultrasensitive sensor for imaging emitted photons from arrayed microspots. It provided suitable signal detectability and spatial resolution for performing accurate measurement for TCL immunoassay with limits of detection in the tens of attomole level. Although in this work the device was employed only for TCL measurements, ongoing work regards the addition of microfluidic connections, to enable integration of a microfluidic chip on which the whole immunoassay can be performed.

In the future, further detector miniaturization is envisaged, exploiting contact imaging configurations avoiding the use of lens and therefore increasing the light collection angle and efficiency. In this case, technical solutions are under development to thermally isolate the microheater and avoid heating of the CCD sensor, which would increase thermal noise and thus reduce detectability. Moreover, as integration of photosensors is a rapidly expanding research field and their suitability for highly sensitive BL/CL measurements was recently shown [32], realization of a fully integrated device is an ongoing work, exploiting thin-film deposition technology for obtaining a disposable glass or plastic support integrating both hydrogenated amorphous silicon photosensors and heaters. This is expected to increase heat transfer and light collection efficiencies, thus lowering measurements times, while increasing detectability.

Employing the portable device for TCL imaging measurements, the analytical performance of biotin-functionalized ORMOSIL/**1**–**4**/BPEA NPs as TCL labels for bioassays was evaluated in a model non-competitive immunoassay for streptavidin, yielding limits of detection in the range 2.5–3.8 ng mL^{-1}, which were comparable to that obtained using conventional enzyme-catalyzed CL detection (0.8 ng mL^{-1}). The excellent detectability of the doped ORMOSIL NPs combined with their easy surface functionalization makes these luminescent NPs ideal candidates as efficient TCL labels. Biotin-ORMOSIL/**1**–**4**/BPEA NPs can be used in the recognition of streptavidin-labeled biomolecules employing simple analytical protocols, because no additional reagents are needed after recognition events and an amplified luminescence signal can be obtained. Moreover, the easy chemical conjugation of the organic groups of ORMOSIL NPs makes it possible to introduce on their surfaces other biospecific probes (such as antibodies, gene probes, aptamers, etc.) to detect a wider range of analytes or even to produce multi-functional nanoprobes.

Thus, TCL NPs could represent a universal reagentless detection system for ultrasensitive bioassays in miniaturized microfluidic formats for life sciences, environmental analysis, and point-of-care testing, as well as for microscopy luminescence imaging of tissues and single cells. Indeed, a reagentless system would allow simplifying instrument design and shortening analytical procedures, as well as (in imaging measurements) avoiding the degradation of image quality due to the presence of a reagent solution on the imaged sample. Additionally, a highest spatial resolution can be achieved employing TCL labels with respect to CL detection, in which the reaction occurs in solution and thus partial resolution loss is caused by diffusion of reaction intermediates. Finally, the availability of this new detection principle in addition to fluorescence, BL, CL, and ECL will enlarge the possibility of multiplexing luminescence-based assays.

We are currently investigating other 1,2-dioxetane derivatives and fluorescence energy acceptors in order to further increase the intensity of TCL emission of doped ORMOSIL NPs, thus exceeding the detectability offered by CL enzyme labels.

Acknowledgments This work was supported by the University of Bologna (FARB Programme), MIUR, and the 2007–2013 Emilia Romagna Regional Operational Programme (ROP) of the European Regional Development Fund (ERDF).

References

1. Roda A, Guardigli M (2012) Analytical chemiluminescence and bioluminescence: latest achievements and new horizons. Anal Bioanal Chem 402:69–76
2. Richter MM (2004) Electrochemiluminescence (ECL). Chem Rev 104:3003–3036
3. Mirasoli M, Guardigli M, Michelini E, Roda A (2014) Recent advancements in chemical luminescence-based lab-on-chip and microfluidic platforms for bioanalysis. J Pharm Biomed Anal 87: 36–52
4. Luider TM, Hummelen JC, Koek JN, Oudman D, Wynberg H (1990) In: van Dyke K, van Dyke R (eds) Luminescence immunoassay and molecular applications. CRC Press, Boca Raton
5. Hummelen JC, Luider TM, Wynberg H (1986) Stable 1,2-dioxetanes as labels for thermochemiluminescent immunoassay. Methods Enzymol 133:531–557
6. Hummelen JC, Luider TM, Wynberg H (1988) In: Collins WP (ed) Complementary immunoassays. John Wiley & Sons, Chichester
7. Roda A, Di Fusco M, Quintavalla A, Guardigli M, Mirasoli M, Lombardo M, Trombini C (2012) Dioxetane-doped silica nanoparticles as ultrasensitive reagentless thermochemiluminescent labels for bioanalytics. Anal Chem 84:9913–9919
8. Di Fusco M, Quintavalla A, Trombini C, Lombardo M, Roda A, Guardigli M, Mirasoli M (2013) Preparation and characterization of thermochemiluminescent acridine-containing 1,2-dioxetanes as promising ultrasensitive labels in bioanalysis. J Org Chem 78: 11238–11246
9. Miralles V, Huerre A, Malloggi F, Jullien M-C (2013) A review of heating and temperature control in microfluidic systems: techniques and applications. Diagnostics 3:33–67
10. Wu J, Kodzius R, Cao W, Wen W (2013) Extraction, amplification and detection of DNA in microfluidic chip-based assays. Microchim Acta 181:1611–1631
11. Marzocchi E, Grilli S, Della Ciana L, Prodi L, Mirasoli M, Roda A (2008) Chemiluminescent detection systems of horseradish peroxidase employing nucleophilic acylation catalysts. Anal Biochem 377: 189–194
12. Roy I, Ohulchanskyy TY, Pudavar HE, Bergey EJ, Oseroff AR, Morgan J, Dougherty TJ, Prasad PN (2003) Ceramic-based nanoparticles entrapping water-insoluble photosensitizing anticancer drugs: a novel drug-carrier system for photodynamic therapy. J Am Chem Soc 125:7860–7865
13. Jain TK, Roy I, De TK, Maitra AN (1998) Nanometer silica particles encapsulating active compounds: a novel ceramic drug carrier. J Am Chem Soc 120:11092–11095
14. Bonacchi S, Genovese D, Juris R, Montalti M, Prodi L, Rampazzo E, Zaccheroni N (2011) Luminescent silica nanoparticles: extending the frontiers of brightness. Angew Chem Int Ed 50:4056–4066
15. Roy I, Ohulchanskyy TY, Bharali DJ, Pudavar HE, Mistretta RA, Kaur N, Prasad PN (2005) Optical tracking of organically modified silica nanoparticles as DNA carriers: a nonviral, nanomedicine approach for gene delivery. Proc Natl Acad Sci USA 102:279–284
16. Hermanson GT (1996) Bioconjugate techniques, 2nd edn. Academic, San Diego
17. Li D, Frey MW, Vynias D, Baeumner AJ (2007) Availability of biotin incorporated in electrospun PLA fibers for streptavidin binding. Polymer 48:6340–6347
18. Roda A, Mirasoli M, Dolci LS, Buragina A, Bonvicini F, Simoni P, Guardigli M (2011) Portable device based on chemiluminescence lensless imaging for personalized diagnostics through multiplex bioanalysis. Anal Chem 83:3178–3185
19. Mirasoli M, Buragina A, Dolci LS, Guardigli M, Simoni P, Montoya A, Maiolini E, Girotti S, Roda A (2012) Development of a chemiluminescence-based quantitative lateral flow immunoassay for on-field detection of 2,4,6-trinitrotoluene. Anal Chim Acta 721: 167–172
20. Mirasoli M, Bonvicini F, Dolci LS, Zangheri M, Gallinella G, Roda A (2013) Portable chemiluminescence multiplex biosensor for quantitative detection of three B19 DNA genotypes. Anal Bioanal Chem 405:1139–1143
21. Lee DC-S, Wilson T (1973) In: Cormier MJ, Hercules M, Lee J (eds) Chemiluminescence and bioluminescence. New York, Plenum
22. Adam W, Heil M (1992) Reaction of 1,2-dioxetanes with heteroatom nucleophiles: adduct formation by nucleophilic attack at the peroxide bond. J Am Chem Soc 114:5591–5598
23. Rao MS, Gray J, Dave BC (2003) Smart glasses: molecular programming of dynamic responses in organosilica sol-gels. J Sol-Gel Sci Technol 26:553–560
24. Atluri R, Sakamoto Y, Garcia-Bennett AE (2009) Co-structure directing agent induced phase transformation of mesoporous materials. Langmuir 25:3189–3195
25. Berlman IB (1971) Handbook of fluorescence spectra of aromatic molecules, 1st edn. Academic, New York
26. Borisevitcha IE, Tabak M (1992) Electronic absorption and fluorescence spectroscopic studies of dipyridamole: effects of solution composition. J Lumin 51:315–322
27. Zaklika KA, Kissel T, Thayer AL, Burns PA, Schaap AP (1979) Mechanism of 1,2-dioxetane decomposition: the role of electron transfer. Photochem Photobiol 30:35–40
28. Menger FM, Jerkunica JM, Johnston JC (1978) The water content of a micelle interior. The Fjord vs. Reef models. J Am Chem Soc 100: 4676–4678
29. Casal HL (1988) On the water content of micelles: infrared spectroscopic studies. J Am Chem Soc 110:5203–5205
30. Kuhn H, Breitzke B, Rehage H (1998) The phenomenon of water penetration into sodium octanoate micelles studied by molecular dynamics computer simulation. Colloid Polym Sci 276:824–832
31. Zaklika KA, Burns PA, Schaap AP (1978) Enhanced chemiluminescence from the silica gel catalyzed decomposition of a 1,2-dioxetane. J Am Chem Soc 100:318–320
32. Mirasoli M, Nascetti A, Caputo D, Zangheri M, Scipinotti R, Cevenini L, de Cesare G, Roda A (2014) Multiwell cartridge with integrated array of amorphous silicon photosensors for chemiluminescence detection: development, characterization and comparison with cooled-CCD luminograph. Anal Bioanal Chem 406:5645–5656